Electronic Supplementary Material (ESI) for RSC Advances
This journal is © The Royal Society of Chemistry 2014

Supporting Information

Cyanide Selective *off-on* Fluorescent Chemosensor with *in-vivo* Imaging in 100% Water: Solid Probe Preferred over *in-situ* Generation

Sanju Das,[a,b] Surajit Biswas,[a] Santanu Mukherjee,[c] Jaya Bandyopadhyay,[c] Subhodip Samanta,[b] Indrani Bhowmick,[d] Dipak Kumar Hazra,[e] Ambarish Ray*[b] and Partha Pratim Parui*[a]

[a]Department of Chemistry, Jadavpur University, Kolkata 700032, India, Fax: +91-33-24146223, Phone:+91-9433490492, E-mail: parthaparui@yahoo.com; [b]Department of Chemistry, Maulana Azad College, Kolakta 700013, India, Fax: +91-33-22268111, Phone:+91-9836650180, E-mail: r_ambarish@yahoo.co.in; [c]Department of Biotechnology, West Bengal University of Technology, Kolkata 700064, India; [d]Department of Chemistry, University of Delhi, Delhi 110007, India; [e]Department of Solid State Physics, Indian Association for the Cultivation of Science, Kolkata 700032, India.

Contents

1. Synthesis and experimental Section

A. Materials: Unless otherwise mentioned, chemicals and solvents were purchased from Sigma-Aldrich Chemicals Private Limited and were used without further purification. Mili-Q Milipore®18.2 MΩ cm^{-1} water was used throughout all the experiments.

B. Syntheses: Caution! *Since the perchlorate salts are potentially explosive, only small amounts of the materials should be handled with care.*

Synthesis of HHMB: 2-hydroxy-3-(hydroxymethyl)-5-methylbenzaldehyde (**HHMB)** was reported earlier without providing detailed analytical measurements.[1] We prepared it with some additional modifications and obtained much better yield. Briefly, 2,6-bis(hydroxylmethyl)-4-methylphenol (8 g, 48 mmol) was dissolved in 500 ML ultra dry chloroform-toluene mixed solvent (1:1, *v*/*v*) under constant stirring condition. Activated MnO_2 (25.6 g, 294.4 mmol) was added portion wise to the stirred solution. The stirring mixture became black and the stirring was continued for next 48h at room temperature. Then the reaction mixture was filtered and washed properly with dry mixed solvent. The filtrate was evaporated under reduced pressure to obtain the crude product. It was purified by column chromatography followed by rotary evaporation and further recrystallized from toluene-chloroform mixed solvent (8:2, *v*/*v*) to afford light yellow colored solid. Yield: 59.8% with respect to the starting phenolic precursor. Anal. cal'd for $C_9H_{10}O_3$: C, 65.05; H, 6.07; obs'd C, 65.10; H, 6.13; %. m.p.: 72°C. Selected IR in cm^{-1} (KBr): 3290 (br), 2918 (m), 2855(m), 1645 (s), 1456 (s), 1253 (s), 1121 (s). ^{1}H NMR ($CDCl_3$, 300MHz): δ = 2.32 (s, 3 H, $ArCH_3$), 4.71 (s, 2 H, CH_2), 7.27 (s, 1 H, ArH), 7.39 (s, 1 H ArH), 9.84 (s, 1 H, CHO), 11.15 (s, 1 H, ArOH) ppm. ^{13}C NMR ($CDCl_3$, 75 MHz): 20.21, 59.99, 120.02, 129.02, 129.10, 132.47, 136.75, 157.10, 196.69.

Synthesis of $Cu(BP)(ClO_4)_2.2H_2O$: It was prepared by the drop wise addition of methanolic solution of 2, 2'-bipyridine (BP) to aqueous $Cu(ClO_4)_2$ solution in equimolar proportion under stirring condition. Recrystallized product was air dried at room temperature. Yield: 78% with respect to starting bpy. Anal. cal'd for $C_{10}H_{12}N_2O_{10}Cl_2Cu$: C, 26.42; H, 2.66; N, 6.16; obs'd C, 26.91; H, 2.89; N, 6.73; %. Selected IR in cm^{-1} (KBr): 3440 (br), 3050(m),3032(m),1601 (s), 1568 (s), 1472 (s), 1023 (s).

Synthesis of $[Cu(BP)HMB]_2(ClO_4)_2$ (1): To an aqueous methanolic solution of **HHMB** (0.249 g, 1.5 mmol), NaOH (0.060 g, 1.5 mmol) was added drop wise with constant stirring. After five minutes, $Cu(BP)(ClO_4)_2.2H_2O$ (1.132 g, 1.5 mmol) was added to it and the mixture was refluxed for 3 h. The solution was then cooled and the precipitate was filtered off. The green colored filtrate was allowed to undergo slow evaporation at ambient temperature in open air. After several weeks, dark green shiny crystals of **1** suitable for X-ray study were obtained from the filtrate and washed with cold methanol followed by diethyl ether and dried in air at room temperature. Yield: 52% with respect to starting **HHMB.** Anal. cal'd for $C_{38}H_{34}N_4O_{14}Cl_2Cu_2$: C, 47.12; H, 3.54; N, 5.78 ; obs'd C, 48.01; H, 3.39; N, 5.32; %. Selected IR in cm^{-1} (KBr): 3434 (br), 1609 (s), 1534 (s), 1384 (m), 1121 (s).

C. Experimental Section:

i) UV-Vis absorption, steady state and time resolved fluorescence: Absorbance spectra were measured with Shimadzu UV-1601PC spectrophotometer. Fluorescence spectra were recorded on a Shimadzu RF-5301-PC spectrophotometer. Emission spectra were recorded by 440-nm excitation. Time-resolved fluorescence measurements were carried out by using time-correlated-single photon-counting (TCSPC) techniques. The nanosecond diode (nano-LED; IBH, U. K) as the light source at 450 nm was used as the excitation source and a TBX4 detection module (IBH, U.K.) coupled with a special Hamamastu photomultiplier tube (PMT) was used for the detection of the fluorescence decays. The time resolution achievable with the present setup following deconvolution analysis of the fluorescence decays was ~ 100 ps. Fluorescence decays were recorded with a vertically polarized excitation beam and fluorescence was collected at the magic angel 54.7˚. All spectroscopic measurements were repeated at least three times to check the reproducibility.

ii) ESI-MS, NMR, CHN, IR, pH and Fluorescence Microscopy: The ESI-MS were recorded on a Waters Qtof Micro YA263 mass spectrometer.in the positive mode. ^{1}H and ^{13}C NMR were recorded in CDCl3 on a Bruker 300 MHz NMR Spectrophotometer using tetramethylsilane (δ = 0) as an internal standard. Elemental analyses were carried out using a Perkin-Elmer 240-elemental analyzer. IR spectra were recorded from KBr pellets with a Perkin-Elmer Spectrum 2 spectrophotometer. pH measurements were performed with Systronics digital pH meter (Model No. 335). Melting point was checked on a programmable melting point apparatus (Model No. VMP-AD) .The bio-imaging were carried out with an Olympus BX51 Fluorescence microscope with a CoolSNAP Pro camera (Media Cybernetics)

iii) X-Ray Crystallography: X-ray diffraction data for **1** was collected at 120(2) K on a Bruker SMART APEX CCD X-ray diffractometer using graphite-monochromated MoKα radiation (λ = 0.71073Å). Determination of integrated intensities and cell refinement were performed with the SAINT software package using a narrow-frame integration algorithm.[2] An empirical absorption correction was applied (SADABS).[2] The structure was solved by direct methods and refined by the full-matrix least-squares technique on F^2 with anisotropic thermal parameters for all non-hydrogen atoms using the programs SHELXS97[3] and SHELXL97.[4] All hydrogen atoms were located from difference Fourier maps and treated with suitable riding models having isotropic displacement parameters derived from their carrier atoms, except the hydrogen atoms of methylene (C19) and hydroxyl (O7) moieties, which were refined with isotropic thermal parameters. A summary of crystal data and relevant refinement parameters for complex **1** is provided in Table S1.

2. Description of the crystal structure: Single crystal structure analysis revealed that the complex **1** crystallizes in the space group $P\bar{1}$ with Z=2. The asymmetric unit of the complex consists of discrete [Cu(BP)**HMB**] with one uncoordinated perchlorate anion. The dimeric unit of **1** consists of [Cu(BP)**HMB**]$_2$, bridged by the oxygen atom (O7) of hydroxylmethyl group. The coordination geometry around the Cu(II) center adopts a (4+1) square pyramid with geometrical factor[5] τ = 0.02. The basal plane is constructed by two nitrogen atoms (N1 and N2) of BP and two oxygen atoms (O5: aldehydic and O6: phenolate) from **HHMB** moiety and the remaining oxygen atom (O7) from hydroxylmethyl group of adjacent **HHMB** moiety occupy the axial site. Selected bond distances and angles around the metal center are listed in Table S2.

Table S1: Crystal structure data and refinement parameters of 1.

Empirical formula	C_{38} H_{34} $N_4O_{14}Cl_2Cu_2$
Formula weight	968.67
Temperature (K)	120(2)
Wavelength (Å)	0.71073
Crystal system	Triclinic
Space group	$P\bar{1}$
a, b, c (Å)	7.9894(5), 10.0752(6), 12.0845(6)
α, β, γ (°)	98.840(2), 100.429(2), 94.519(2)
Volume (Å^3)	939.60(9)
Calculated density (Mgm^{-3})	1.712
Absorption coefficient (mm^{-1})	1.352
F(000)	494
θ range for data collection (°)	2.06 to 24.76
Limiting indices	$-9 \le h \le 9$, $-11 \le k \le 11$, $-14 \le l \le 13$
Reflections collected / unique	7082 / 3191 [R(int) = 0.0219]
Completeness to 2θ (%)	98.6
Refinement method	Full-matrix least-squares on F^2
Data / restraints / parameters	3191 / 1 / 284
Goodness-of-fit on F^2	1.099
Final R indices [I>2σ(I)]	R_1 = 0.0331, wR_2 = 0.0887
R indices (all data)	R_1 = 0.0354, wR_2 = 0.0942
Largest diff. peak and hole (e.Å^{-3})	0.681 and -0.542

Table S2: Selected bond lengths (Å) and angles (°) for 1

Cu(1) – N(1)	1.986(2)
Cu(1) – N(2)	1.990(2)
Cu(1) – O(5)	1.940(2)
Cu(1) – O(6)	1.893(2)
Cu(1) – O(7)*	2.311(2)
N(2) – Cu(1) – N(1)	81.61(9)
O(5) – Cu(1) – O(6)	93.88 (8)
O(5) – Cu(1) – N(2)	169.18(9)
O(5) – Cu(1) – N(1)	91.25(9)
O(6) – Cu(1) – N(1)	171.32(8)
O(6) – Cu(1) – N(2)	92.28(9)
O(5) – Cu(1) – O(7)*	92.22(8)
O(6) – Cu(1) – O(7)*	93.64(8)
N(1) – Cu(1) – O(7)*	93.15(8)
N(2) – Cu(1) – O(7)*	96.25(8)

*-x,-y,-z

3. Determination of detection limit:

The limit of detection (LOD) for the CN^- concentration by fluorescence measurement was determined from the following equation with reasonable certainty: [6]

$$\mathrm{LOD}\left(CN^-\right) = K \times s_{bi} \times S \qquad (1)$$

Where, K = 3 has been considered as per IUPAC recommendation. s_{bi} = standard deviation for the blank measurement, and S = Δconcentration/Δintensity (the slope of the calibration curve between fluorescence enhancement with change in CN^- concentration).

By using the above equation (1), LOD of CN^- concentration *ca.* 0.7 μM was obtained in 10 mM HEPES buffer at pH 7.4.

4. Determination of fluorescence quantum yield (ϕ_F):

The fluorescence quantum yield of **HHMB** was determined using the standard method[7] (Eq. 2). 9,10-diphenylanthracene in ethanol was used as reference,[8] ϕ_F^r = 0.95.

$$\phi_F^s = [A_r F_s n^2_s / A_s F_r n^2_r]\ \phi_F^r \qquad (2)$$

where, A is the absorbance at the excitation wavelength, F is the integrated emission area and n is the refraction index of the solvents used. Subscripts refer to the reference (r) or sample (s) compound. The **HHMB** fluorescence spectra was recorded by 440 nm excitation at 25ºC in 10 mM HEPES, pH 7.4. By using the above equation (2), ϕ_F *ca.* 0.05 (λ_{ex} = 440 nm) was obtained in aqueous 10 mM HEPES buffer at pH 7.4.

5. Fluorescence studies to monitor *in-situ* complexation:

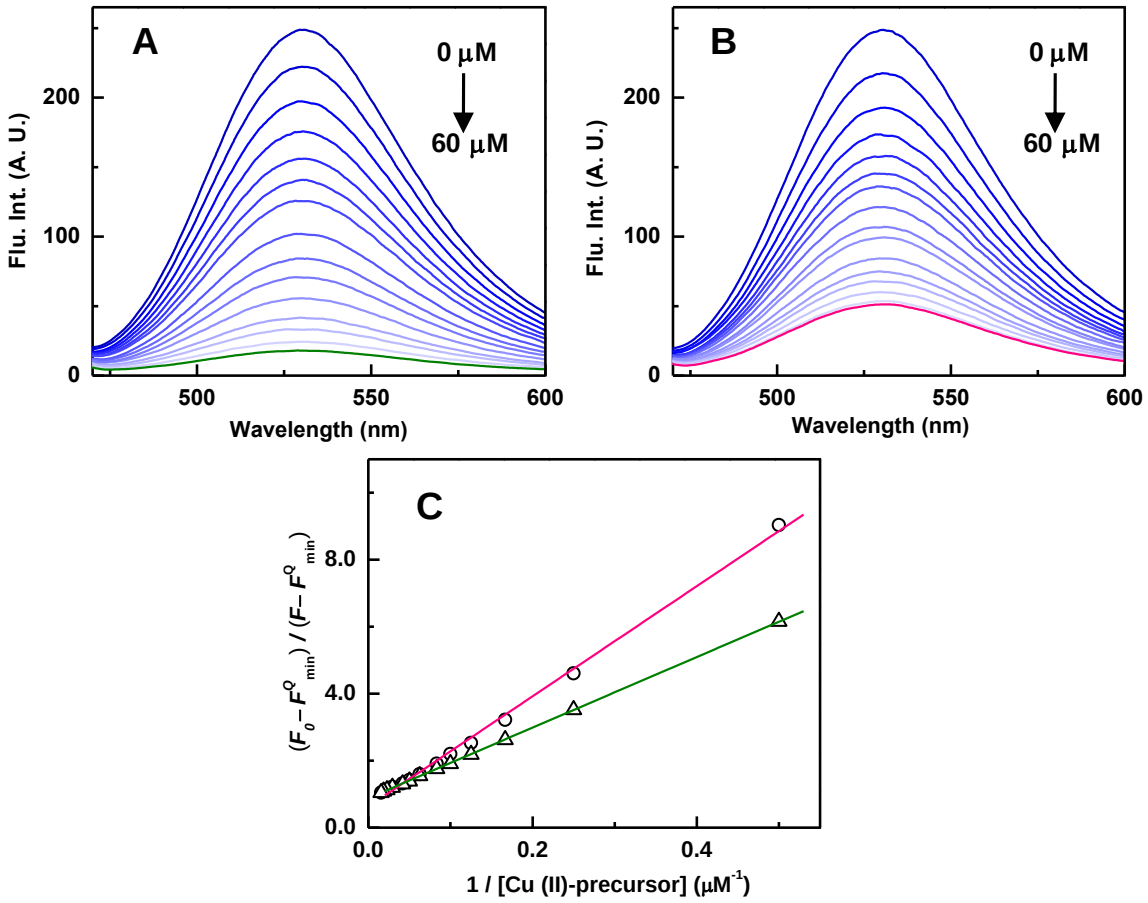

Fig. S1: Fluorescence spectra of **HHMB** (10 μM) in presence of increasing amount of (A) $Cu(BP)(ClO_4)_2$ (0–60 μM) (B) $Cu(ClO_4)_2$ (0–60 μM) in 10 mM HEPES buffer, pH 7.4 at 25ºC; the gradual decrease of emission intensity for different concentrations of Cu(II)-precursors are indicated by the arrows. The saturated fluorescence spectrum in presence of (A) $Cu(BP)(ClO_4)_2$ and (B) $Cu(ClO_4)_2$ are depicted by dark green and pink color, respectively. (C)The Benesi-Hildebrand[9] plot of $(F_0 - F^Q_{min})/(F_0 - F^Q_{min})$ vs. 1/[Cu(II)] for $Cu(ClO_4)_2$ (circle, pink), $Cu(BP)(ClO_4)_2$ (triangle, dark green) are shown. The plots of $(F_0 - F_{min})/(F_0 - F_{min})$ vs. 1/[Cu(II)] show a liner relationship with an intercept of about 0.8 ± 0.1 (close to 1.0) for both Cu(II)-precursors suggesting 1:1 binding stoichiometry. (Excitation wavelength: 440 nm).

6. UV-Vis absorption studies to monitor *in-situ* complexation:

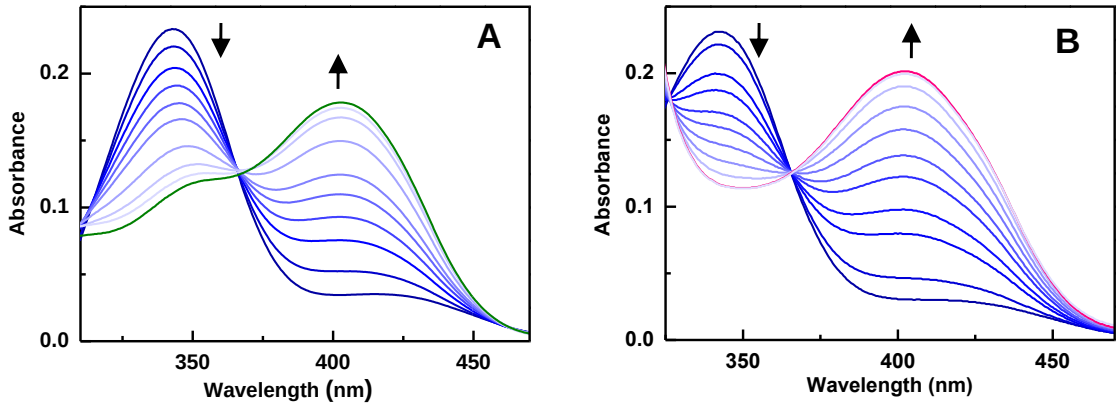

Fig. S2: UV-Vis absorption spectra of **HHMB** (50 μM) in presence of increasing amount of (A) $Cu(ClO_4)_2$ (0–250 μM) (B) $Cu(BP)(ClO_4)_2$ (0–250 μM) in 20 mM HEPES buffer, pH 7.4 at 25°C. The gradual increase or decrease of absorption intensity for different concentrations of Cu(II)-precursors are indicated by the arrows. The saturated absorption spectrum in presence of (A) $Cu(ClO_4)_2$ and (B) $Cu(BP)(ClO_4)_2$ are indicated by dark green and pink color, respectively.

7. DFT and TDDFT calculations:

DFT calculations on free **HHMB** and most probable monomeric structure (**1a**) of **1** were performed using Gaussian 03 program.[10] The B3LYP functional has been adopted along with 6-31++G (d,p) basis set for H, C, N, O atoms and LANL2DZ effective core potentials and basis set for the Cu atom. The global minima of all these species were confirmed by the positive vibrational frequencies. Time dependent density functional theory (TDDFT) [11] with B3LYP density functional was applied to study the low-lying excited states of the free **HHMB** and the monomer **1a** in gas phase as well as in water using the optimized geometries of the ground (S_0) states of respective species. The vertical excitation energies of the lowest 25 singlet states are also computed. The UV spectra computed from TDDFT calculations in the range 250-450 nm in water show quenching of 340 nm peak of **HHMB** and appearance of new 404 nm peak in **1a**. The band around 400 nm is dominated by the HOMO (104A) → LUMO (105A) excitation. This matches with the experimental absorption spectra of **1** in aqueous solution and further supports our proposition for the presence of monomer (**1a**) in aqueous phase. A comparative account of the vertical excitation energies and oscillator strengths of free **HHMB** and **1a** in water are shown in **Table S3**.

Table S3. Vertical excitation energies (E_{cal}) and oscillator strengths (f_{cal}) of the lowest few excited singlets were obtained from TDDFT calculations of free **HHMB** and **1a** in water (ε_k = 78.21).

Compound	E_{cal} (nm)	f_{cal}	Probable monomer	E_{cal} (nm)	f_{cal}
	-	-		404	0.0533
	-	-		393	0.0034
HHMB	-	-	**1a**	376	0.0408
	338	0.0891		340	0.0173
	-	-		316	0.0116
	308	0.1568		314	0.0944
	257	0.1645		299	0.1073

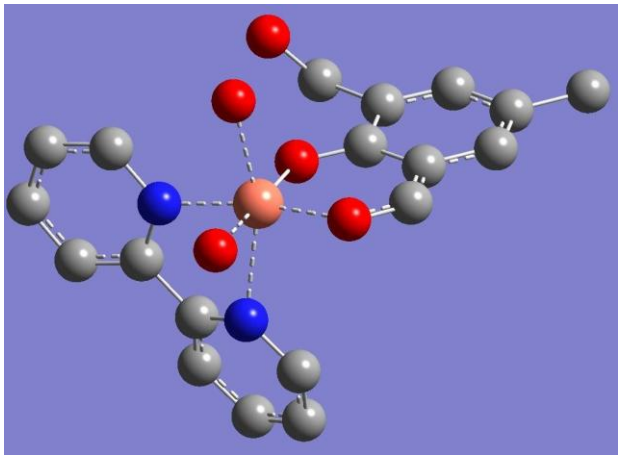

Fig. S3. DFT optimized structure of **1a.** All H-atoms and perchlorate are omitted for clarity.

8. ESI-MS$^+$:

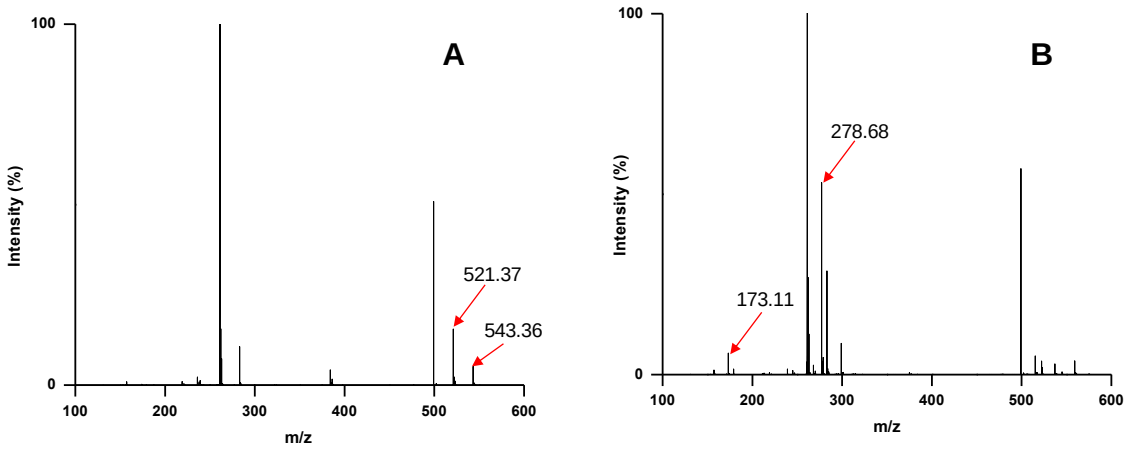

Fig. S4: ESI-MS$^+$ of (A) **1** (*m/z*: obs'd – 521.37 (cal'd 521.39) for [**1a**H]$^+$, obs'd – 543.36 (cal'd 543.37) for [**1a**Na]$^+$) and (B) **1** + CN^- (*m/z*: obs'd – 278.68 (calcd 278.71) for [Cu(BP)$(CN)_2$Li]$^+$, obs'd – 173.11 (cal'd 173.12) for [**HHMB**Li]$^+$) in aqueous 20 mM HEPES buffer, pH 7.4.

9. Job's method for determining the stoichiometry:

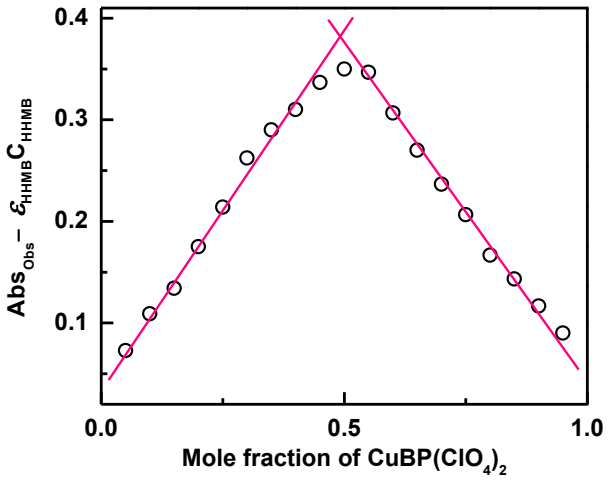

Fig. S5: Job's plot for determining the stoichiometry of the complex between **HHMB** and $Cu(BP)(ClO_4)_2$. The difference between the observed and **HHMB** absorbance at 400 nm were plotted with mole fraction of $Cu(BP)(ClO_4)_2$ in the mixture of **HHMB** and $Cu(BP)(ClO_4)_2$ with various compositions ($\varepsilon_{\mathbf{HHMB}}$ and $C_{\mathbf{HHMB}}$ are the extension coefficient and concentration of **HHMB**, respectively).

10. CN^- sensing in presence of other anion:

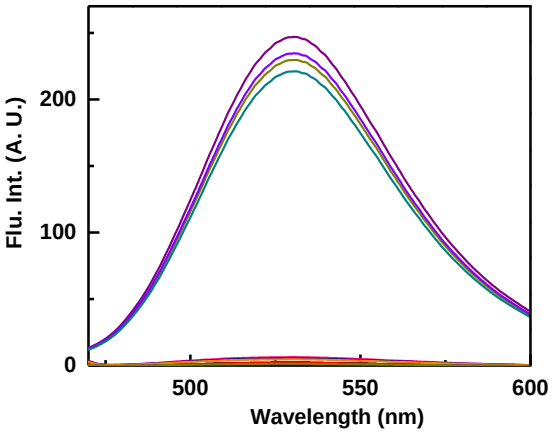

Fig. S6: Fluorescence response of **1** (20 μM) towards different individual anions or molecules (100 μM), or mixture of anions (individual concentration in the mixture, 100 μM) in 10 mM HEPES, pH 7.4 at 25ºC. Color index: CN^- (purple), N_3^- + AcO^- + CN^- (violet), F^- + Cl^- + Br^- + I^- +CN^- (dark yellow), $H_2PO_4^-$ + HPO_4^{2-} + CN^- (cyan). Those other anions or molecules are depicted by different colors.

11. Fluorescence lifetime measurements:

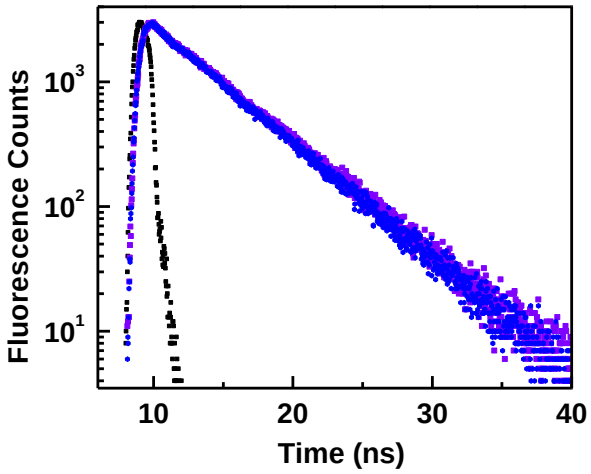

Fig. S7: Fluorescence transients of **HHMB** (20 μM) (blue) and **1** (20 μM) + CN^- (100 μM) (violet) in 10 mM HEPES buffer, pH 7.4. Scattering profile is shown by black curve. The excitation and emission wavelength were 450 nm and 530 nm respectively.

Decay curves for free **HHMB**, complex **1** in presence of 5-equivalent CN^- are fitted mono-exponentially and the obtained decay lifetime of the fluorescent transient are *ca.* 4.8 ns for each cases (χ^2 = 1.02 for both fitting).

12. CN^- induced fluorescence response of Cu(II) complexes:

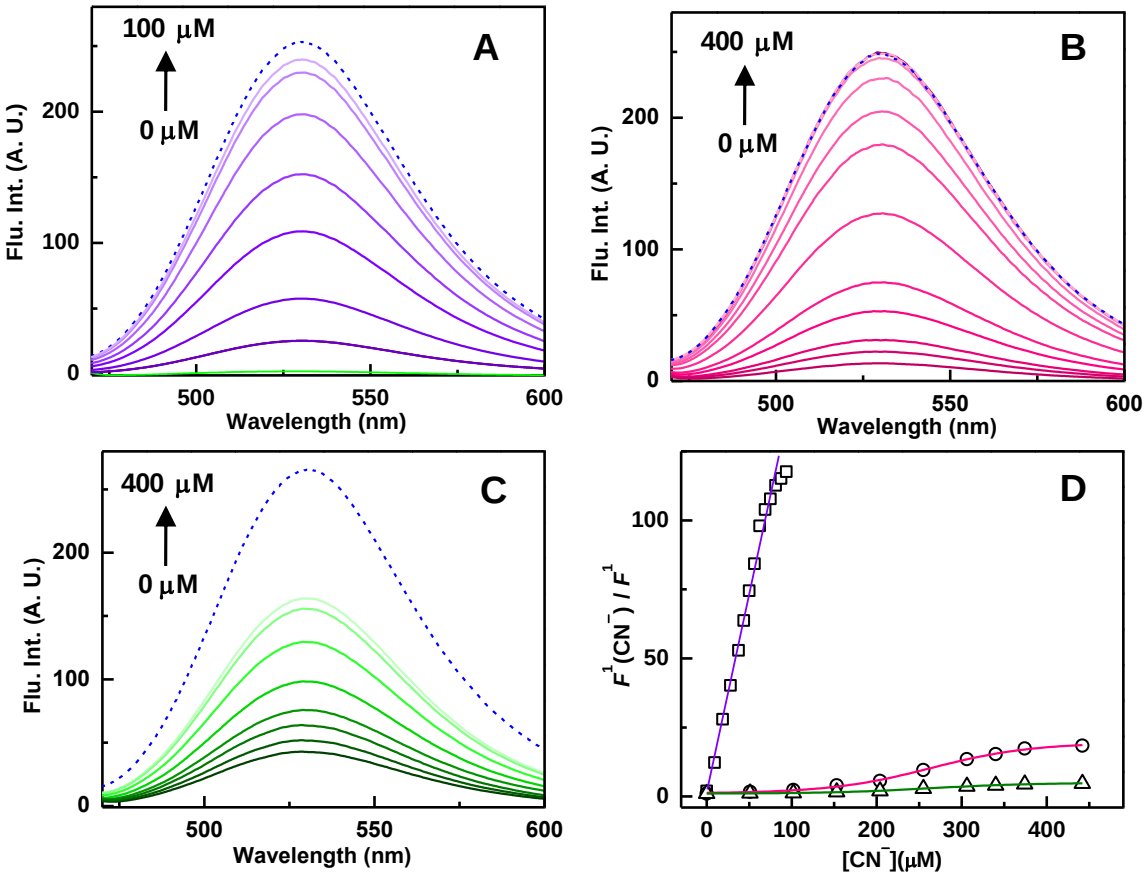

Fig. S8: Fluorescence response of (A) **1** (20 μM), (B) **HHBM** (20μM) + $Cu(BP)(ClO_4)_2$ (120 μM) and (C) HHMB (20μM) + $Cu(ClO_4)_2$ (120 μM) towards increasing concentration of CN^- in 10 mM HEPES, pH 7.4 at 25ºC. The green spectrum (A) is for **1** in absence of CN^-. The increases of fluorescence intensity with concentration of CN^- are depicted by the arrow. (A–C) The dashed blue line is for the **HHMB** (20 μM). (D) The fluorescence intensity ratio between in presence and absence of CN^- are plotted with CN^- concentrations; **1** (purple), **HHBM** (20μM) + $Cu(BP)(ClO_4)_2$ (120 μM) (pink) and **HHMB** (20μM) + $Cu(ClO_4)_2$ (120 μM) (green) at 530 nm. (Excitation wavelength: 440 nm)

13. Effect of pH on ratiometric fluorescence response:

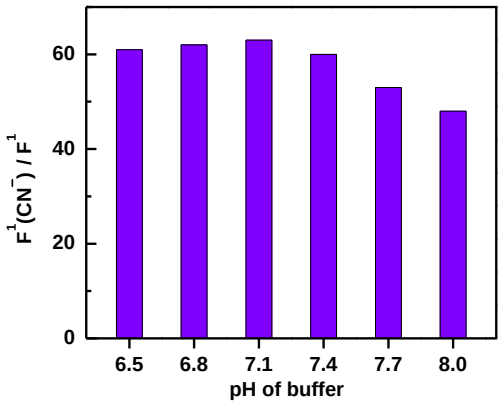

Fig. S9: The fluorescence intensity ratio between in presence and absence of 100 μM CN^- of **1** at 530 nm at different pH of 10 mM HEPES at 25°C are represented with a bar-diagram. (Excitation wavelength: 440 nm).

14. CN^- association with $Cu(BP)(ClO_4)_2$:

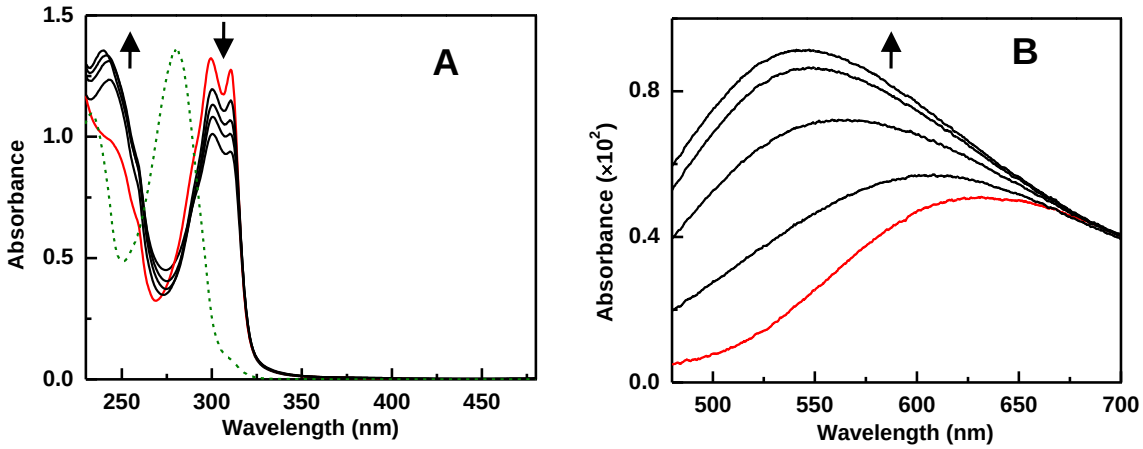

Fig. S10: UV-Vis absorption spectra of $Cu(BP)(ClO_4)_2$ in presence of increasing amount of CN^-. The gradual increase or decrease of absorption intensity with CN^- is indicated by the arrows. (A) Spectra (230–480) of 50 μM $Cu(BP)(ClO_4)_2$ in presence of CN^- (0–250 μM) are shown. The dashed green line is for BP (50 μM). (B) Spectra (480–700) of 100 μM $Cu(BP)(ClO_4)_2$ in presence of CN^- (0–500 μM) are shown. Measurement condition: buffer: (A) 20 mM and (B) 40 mM HEPES, pH: 7.4, temperature: 25ºC.

The CN^- attack at the Cu(II) centre was confirmed from the CN^- induced absorbance change of $Cu(BP)(ClO_4)_2$ both at shorter and longer wavelength region. In presence of 6-equivalent of CN^-, the presence of Cu (II)-associated BP absorption characteristic was observed at around 300 nm with about 25% decrease in intensity. Moreover, generation of free BP from probable dissociation of $Cu(BP)(ClO_4)_2$ was not observed in presence of CN^-. These results indicates that CN^- associated with $Cu(BP)^{2+}(aq)$ to form $[Cu(BP)(CN)_x]^{n-}$ (aq). This proposition was further supported by the CN^- induced d-d absorption changes of $Cu(BP)(ClO_4)_2$ in the visible range spectra.

15. Bio-imaging studies:

Caenorhabditis elegans strain (wild-type N2) and *Escherichia coli* bacterial strains (OP50) were obtained from the *Caenorhabditis elegans* Genetics Center (CGC) at the University of Minnesota, USA. Synchronized nematodes were maintained at 20ºC on OP50 strain-seeded NGM (nematode growth medium) agar plates (0.3% NaCl, 0.25% bacto peptone, 1.7% agar, 5 mg/ml cholesterol, 1 mM $CaCl_2$, 1 mM $MgSO_4$, 25 mM KH_2PO_4). The effect of CN^- on the fluorescence of sensor **1** as well as the *in-situ* complex generated by **HHMB** and $Cu(BP)(ClO_4)_2$ were studied using *C. elegans*. Briefly, solutions of sensor **1 (**20 μM) and in case of the *in-situ* complex, **HHMB (**20μM) + $Cu(BP)(ClO_4)_2$ (100 μM) were freshly prepared using NGM buffer just prior to use. Worms were washed with NGM buffer by centrifuging (800 G) and subsequently aspirated to remove any remaining buffer left behind in the tube. Sensor **1** and in case of the *in-situ* complex, **HHMB (**20μM) + $Cu(BP)(ClO_4)_2$ (100 μM) were applied immediately to the worm pellet. The solution along with the worm pellet was mixed uniformly by gentle tapping of the tubes. Following exposure for 1 h., the worms were washed three times with NGM buffer as described earlier. 10 μL of the solution containing the worms were taken and prepared for microscopic imaging. Separately, 100 μL of worms already exposed to sensor **1** and the *in-situ* complex were transferred to several micro-centrifuge tubes. Various concentrations (each in triplicates) of CN^- (0–100 μM for **1**; 0–400 μM for allied *in-situ* complex) were applied to the worms pre-exposed to the sensor **1** and the allied *in-situ* complex in NGM buffer, tapped gently, and subsequently incubated for 1 h. at 25ºC. Following incubation, the worms were washed three times with NGM buffer before mounting onto a glass slide with a mounting medium (Sigma). The nematodes were visualized with an Olympus BX51 Fluorescence microscope (excitation *ca.* 470 nm) with a CoolSNAP Pro camera (Media Cybernetics).

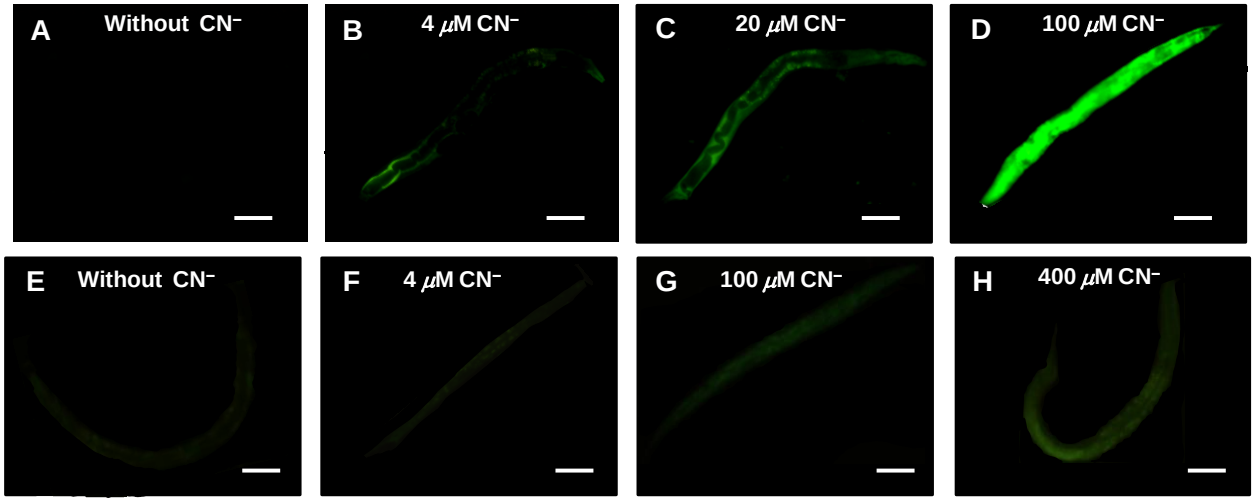

Fig. S11: Fluorescence images of the nematode *C. elegans* exposed to complex **1** (A–D) and *in-situ* complex between **HHMB** and $Cu(BP)(ClO_4)_2$ (E–H) in presence of different CN^- concentration. The phase contrast is identical for all images. The scale bars: 40 μm.

16. Assessment of toxicity of compounds using lethality assays

Lethality assays were conducted with wild-type (N2) *C. elegans* and *daf-2 (e1370)* and *daf-16 (m16)* mutant worms following the methods as described[12] with slight modifications. Experiments were conducted in M9 buffer. Wild type and mutant worms were exposed to higher doses of the compounds (1 mM each final concentration) in 24-well cell culture dishes for 1 h at 25^{o}C. Exposed worms were then transferred to OP-50 seeded NGM plates and scored for dead worms. Each experiment comprised of triplicate sets (n = 10 worms per set) which was repeated twice to reduce experimental variability. No toxicity of compounds was observed for the doses that were exposed to the N2 wild-type worms as evidenced from their 0% lethality rates. However, *daf-2* and *daf-16* mutants displayed slight increase in the lethality rates compared to wild-type worms (**Table S4**) as evidenced from the number of dead worms scored.

Table S4 : Assessment of toxicity of compounds by lethality assays in *C. elegans*

Strain[n]	% dead worms following exposure of compounds	
	Sensor **1** (1 mM)	**HHMB** (1 mM)
N2	0	0
daf-2 (e1370)	17 ± 1	0
daf-16 (m16)	36 ± 1	1

Lethality assays were conducted with wild-type (N2) *C. elegans* and *daf-2 (e1370) and daf-16 (m16)* mutant worms in higher doses of compounds. Experiments were conducted in M9 buffer.
n = A total of 60 worms under each strain were tested for each chemical exposure. Each experiment comprised of triplicate sets (n = 10 worms per set) which was repeated twice.

17(A). ^{1}H NMR figure of HHMB

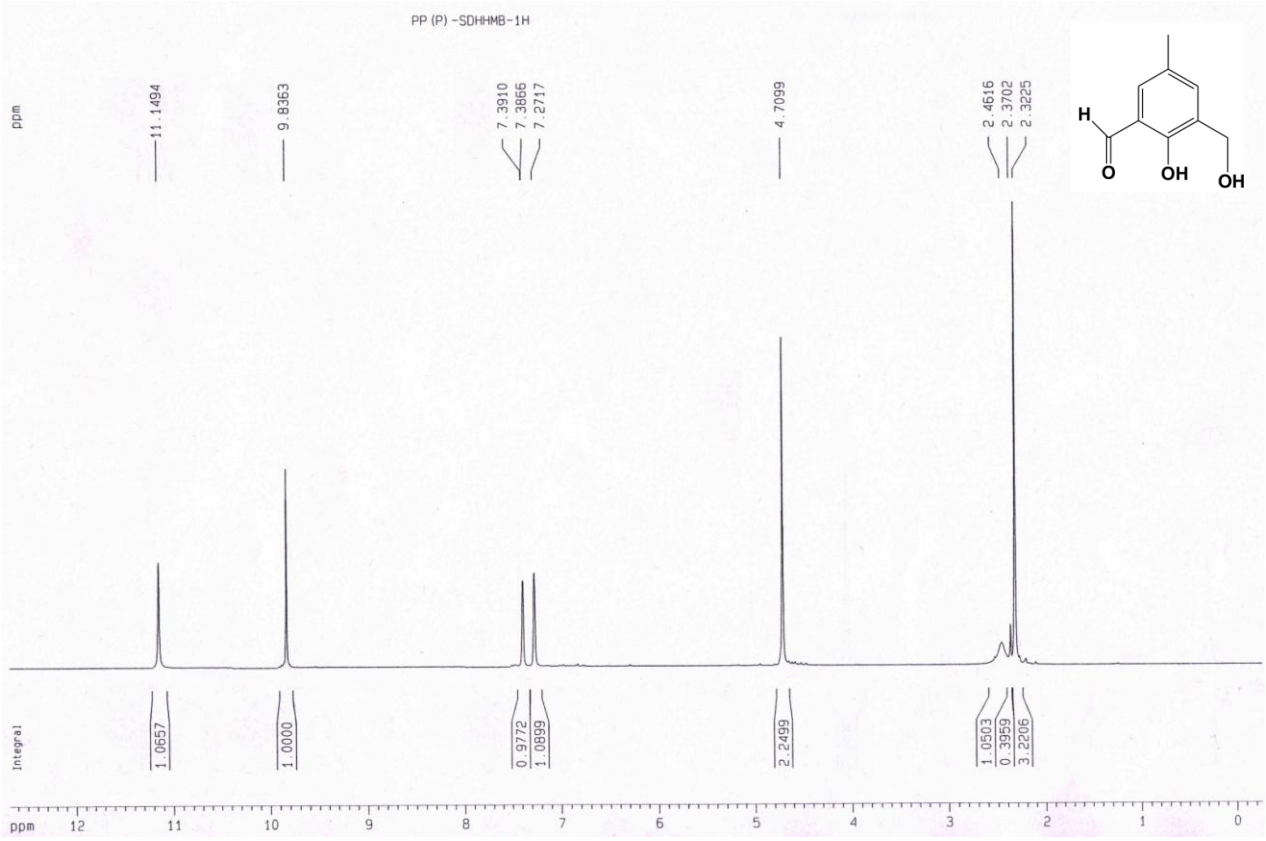

17(A). ^{13}C NMR figure of HHMB

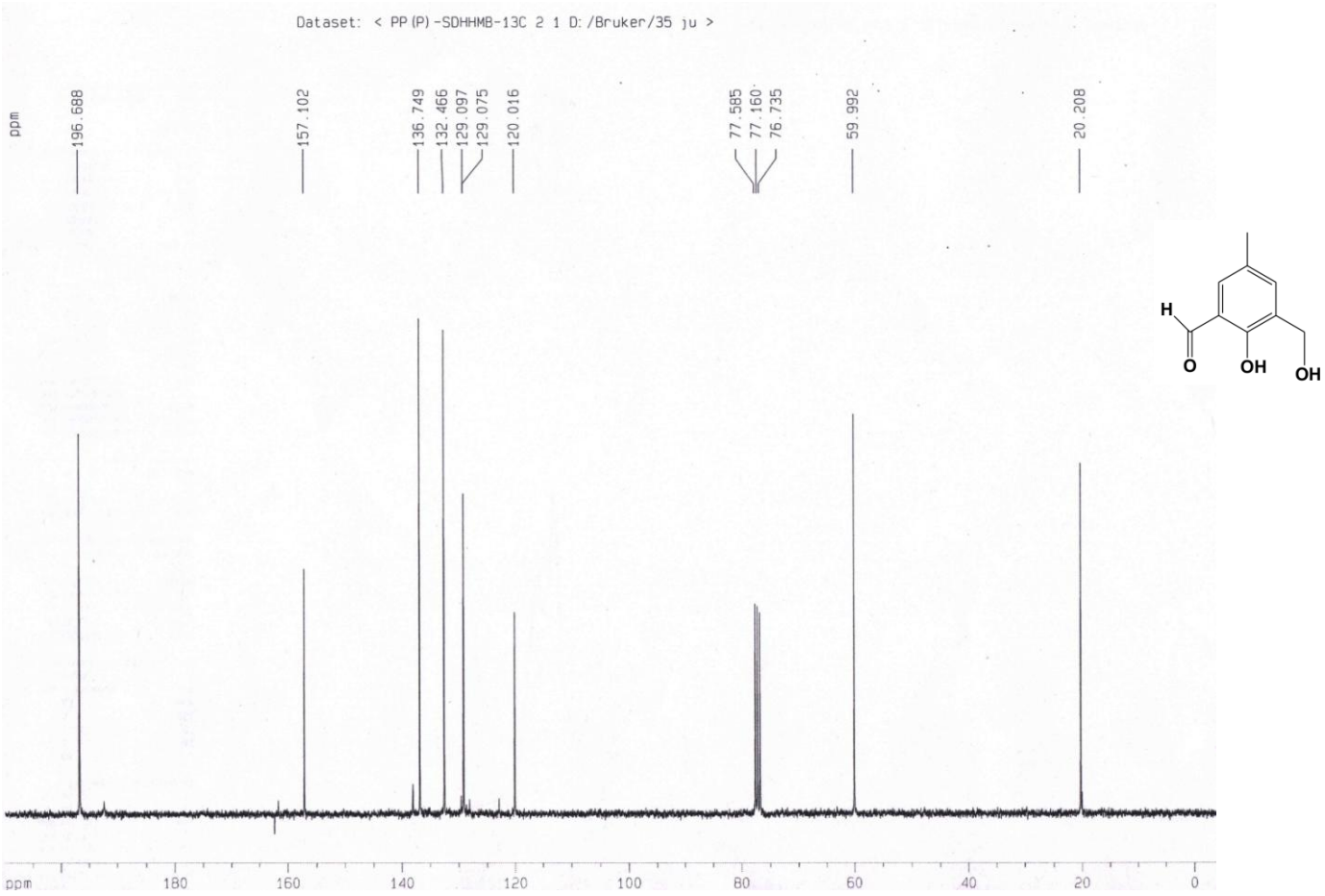

19. References:

1. E. Lambert, B. Chabut, S. C. Noblat, A. Deronzier, G. Chottard, A. Bousseksou, J.-P. Tuchagues, J. Laugier, M. Bardet and J.-M. Latour, *J. Am. Chem. Soc.*, 1997, **119,** 9424.
2. *SAINT (version 6.02)*, *SADABS (version 2.03)*, Bruker AXS Inc., Madison, Wisconsin, 2002.
3. G. M. Sheldrick, *SHELXS-97*, *Program for solution of crystal structures*, University of Göttingen, Germany, 1997.
4. G. M. Sheldrick, *SHELXL97*, *Program for Crystal Structure Refinement*, University of Göttingen, Germany, 1997.
5. M. Ali, A. Ray, W. S. Sheldrick, H. Mayer-Figge, S. Gao and A. I. Shames, *New J. Chem.*, 2004, **28**, 412.
6. V. Thomsen, D. Schatzlein and D. Mercuro, *Spectroscopy*, 2003, **18**, 112.
7. J. N. Demas and G. A. Crosby, *J. Phys. Chem.*, 1971, **75**, 991.
8. J. V. Morris, M. A. Mahaney and J. R. Huber, *J. Phys. Chem.*, 1976, **80**, 969.
9. H. A. Benesi and J. H. Hildebrand , *J. Am. Chem. Soc.*, 1949, **71,** 2703.
10. M. J. Frisch *et al*., *Gaussian 03, revision C. 02*, Gaussian, Inc., Wallingford, CT, 2004.
11. (a) S. Miertus, E. Scrocco and J. Tomasi, *Chem. Phys.*, 1981, **55**, 117; (b) V. Barone, M. Cossi and J. Tomasi, *J. comput. Chem.*, 1998, **19**, 404.
12. M. Dengg and J.C.A. van Meel, *J. Pharmacol. Toxicol. Methods*, 2004, **50**, 209.